ACERP: Vol. 1, No. 4 (Winter 2016) 19-25

Advanced Ceramics Progress

Research Article

Journal Homepage: www.acerp.ir

Enhanced Physical Properties of Indium Tin Oxide Thin Films: Effect of Zinc Oxide Buffer Layer

N. Manavizadeh

Faculty of Electrical Engineering, K. N. Toosi University of Technology, Tehran, Iran.

PAPER INFO

Paper history:
Received 22 November 2015
Accepted in revised form16 February 2016

Keywords:
ITO thin films
ZnO
Buffer layer
Structural properties
Electrical and optical properties

This study investigates the structural, electrical and optical properties of indium tin oxide or ITO (In_2O_3:SnO_2) thin films on galss, mono and multicrustalline silicon substrates. A 100-nm-thick zinc oxide (ZnO) buffer layer is utilized to simultaneously improve the electrical and optical properties of ITO films. High quality ZnO and ITO layers are deposited by a radio frequency sputtering in argon ambient with plasma powers of 150 W and 300 W, respectively. After deposition, samples are annealed in a high vacuum furnace at 400 ˚C. The effects of ZnO-coated substrates on the crystallinity and morphological properties of ITO films are analyzed by X-ray diffractometer, field emission scanning electron microscopy (FESEM) and atomic force microscopy (AFM). X-ray diffraction patterns confirm the hexagonal wurtzite type polycrystalline structure of the ZnO films. FESEM and AFM analyses indicate that applying the ZnO buffer layer affects the surface morphology of the ITO films. Results also reveal that the roughness of ITO thin films is decreased in presence of the ZnO buffer layers. Moreover, it has been found that ZnO incorporation promotes the crystal properties of the ITO layer by reducing its resistivity without deteriorating the optical transmittance.

ABSTRACT

1. INTRODUCTION

Transparent conducting materials like indium tin oxide (ITO) films have been extensively studied in the past few years. Their high electrical conductivity, prominent visible transmittance, and significant infrared reflectance make these films have numerous industrial applications, such as solar cells, liquid crystal displays, and energy efficient windows [1,2].

High-quality ITO thin films can be realized by using various deposition processes: radio frequency (RF) and DC sputtering, electron beam evaporation, pulsed laser deposition, and spray pyrolysis. Due to the low process temperatures and more controllable stoichiometry of the obtained films, sputtering is a more suitable technique [3]. Optical and electrical properties of ITO thin films strongly depend on the defect density created by disturbed stoichiometry as well as film preparation, substrate nature, and the annealing procedures [4]. Moreover, the electrical behavior also varies with the amount of substitutional tin atoms and oxygen vacancies [4,5]. The oxygen nonstoichiometry improves the conductivity of the material by providing two electron carriers per oxygen vacancy, while doping with Sn^{4+} ions introduces one free electron [6]. The conductivity can be increased further by reductive annealing of the as-deposited ITO layers due to an increase in carrier mobilities. However, lowering the oxygen content of the ITO layer degrades the transparency of the film. Hence, there is a trade-off between electrical and optical characteristics of ITO films for optoelectronic applications.

On the other hand, zinc oxide (ZnO) is a compound semiconductor with a wurtzite structure and has a wide direct band gap of 3.37 eV at room temperature. It is naturally an n-type semiconductor due to deviation from stoichiometry. The free charge carriers mainly arise from the shallow donor levels associated with the oxygen vacancies and interstitial zinc atoms [5].

It is reported that multilayer thin films comprise different physical properties in comparison with the monolayer thin films [7,8]. Thin films deposited on buffer layer-coated substrates have higher quality than those deposited on bare substrates [7-9]. Herrero and Guillén demonstrated that the crystallinity of ITO films on soda-lime glass substrates can be improved by

*Corresponding Author's Email: manavizadeh@kntu.ac.ir

utilizing a ZnO buffer layer [9]. In addition to the better crystalline structure, the (0002) preferred orientation of the ZnO promotes the ITO grain size, which reduces the electron scattering and improves the electrical conductivity. Furthermore, Seong et. al. investigated the effect of ZnO buffer layers on the crystallinity of the ITO thin films as a function of the buffer layer thickness and showed that an increase in the ZnO thickness could improve the properties of the ITO thin films [10].
The photovoltaic (PV) research and industry must have lower costs and higher efficiency in future. Therefore, a large variety of possible and viable methods for manufacturing low-cost solar cells are being investigated. Among them, transparent conductive oxides and polycrystalline silicon thin films are two strategies which are considered promising and challenging, respectively for application of PV and development of cheap TCOs and TCO/c-Si heterojunction cells [11,12]. Therefore, in this paper, the impact of structural, electrical and optical properties of ITO films on monocrystalline silicon (c-Si) wafers, multi-crystalline silicon (mc-Si) wafers, and glass substrates is systematically investigated regarding the ZnO buffer layer

2. METEDOLOGY

The substrates used in this study were micro slide glass, p-type (100) c-Si, and textured mc-Si with thicknesses of about 150 µm, 500 µm, and 300 µm, respectively. All substrates were degreased and cleaned by RCA SC-1 method (deionized water, ammonia solution, hydrogen peroxide 5:1:1) [13]. Afterwards, the Si wafers were dipped in 10% HF solution to remove the native oxide layer and then rinsed in deionized water [13]. A 100-nm-thick layer of ZnO was deposited on all substrates. The thickness of the layers was measured by alpha-step (Dektak 500). The deposition of the ZnO film was performed in an RF diode sputtering unit using a 3-inch-diameter ZnO source with 99.99% purity, at a base pressure of 6×10^{-6} Torr. The deposition process was carried out at plasma power of 150 W in high purity argon (99.999%) ambient with a pressure of 20 mTorr. Subsequently, an ITO layer with a thickness of 300 nm was deposited over the ZnO-coated substrates using the same sputtering unit. The deposition was executed using an oxide ceramic target (99.99% purity) composed of 90 wt.% In_2O_3 and 10 wt.% SnO_2 with a plasma power of 300 W and pressure of 20 mTorr. Samples were then annealed at 400˚C in high vacuum at 5×10^{-5} Torr [14]. Annealing in an oxygen-deficient atmosphere not only promotes crystalline growth, but it also increases the carrier concentration of ITO by creation of oxygen-vacancy [15]. In order to study the crystalline structure of the thin films, X-ray diffraction analysis (XRD) was performed using a PW 1050/25 Philips diffractometer equipped with proportional counter and discriminator as well as an N-filtered Cu radiation at 40 kV and 20 mA apparatus. A Hitachi S-4160 field emission scanning electron microscope (FESEM) operating at 20 kV was used to study surface morphology and cross sectional imaging of the layers. Surface topographies of the layers were also investigated by a silicon tip NT-MDT NEXT Solver atomic force microscope (AFM) operating in non-contact mode. The optical properties of the films were examined by the use of a Varian Cary 500 UV/VIS/IR spectrometer, and the electrical properties were measured by a four point probe apparatus (Keithley 196 and 224).

3. RESULTS AND DESCUSSION

In order to scrutinize the influence of the ZnO buffer layer on the electrical and optical properties of the subsequent ITO layer, the impact of the properties of ITO layers on bare and ZnO-coated substrates were analyzed. In this study, the thickness of the ITO layer and that of the ZnO buffer layer were fixed at 300 nm and 100 nm, respectively. The impact of the structure of ZnO layers on silicon wafers and glass substrates was investigated prior to the ITO deposition.

3.1. STRUCTRUAL PROPERTIES OF ZnO

The purpose of utilizing the ZnO buffer layer is to obtain highly transparent conductive ITO films. Hence, the ZnO buffer layer is required to be single c-axis oriented (highly textured) and electrically insulating (not to interfere with optical and electrical characteristics of the subsequent ITO layer) [5]. It has been reported that ZnO films naturally show a strong (0002) preferred orientation in a wide range of deposition conditions, with their electrical resistivity mainly depending on the oxygen content [16,17].

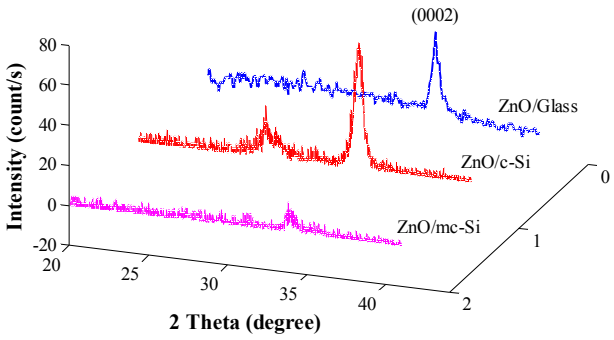

Figure 1. XRD patterns of ZnO thin film on multi-crystalline Si wafer, monocrystalline Si wafer, and glass substrate [18]

The XRD measurement of the 100-nm-thick ZnO films deposited on different substrates and annealed at 400˚C is shown in Figure 1, corresponding to the card number JCPDS 36-1451 of hexagonal wurtzite phase of ZnO. The XRD spectra of all three specimens demonstrate strong peaks, which corresponded to the diffraction of the <0002> preferred orientation of the hexagonal wurtzite ZnO with the c-axis perpendicular to the substrate. As shown in Figure 1, the (0002) peak is the highest for the ZnO layer deposited on c-Si substrate. Comparing to the standard [0002] peak occurring at 2θ = 34.43˚, a slight shift is observed in the XRD spectra indicating the formation of defects in the films. The average size of the crystalline grains can be extracted from the XRD results using Debye–Scherrer formula (Eq. 1) [19]:

$$D_{hkl} = \frac{0.9\lambda}{\beta \cos\left(\theta_{hkl}\right)} \quad (1)$$

where λ is the X-ray wavelength, θ_{hkl} is the Bragg diffraction angle and β (in radian) is the full width at half maximum of the main peak in the XRD pattern. The calculated crystallite sizes are summarized in Table 1.

Figure 2 demonstrates plan-view and cross-sectional SEM images of ZnO films on various substrates. As shown in this figure, ZnO films on mc-Si substrates have larger grain sizes than those on glass and c-Si substrates, which is in consistent with the results obtained from the Debye–Scherrer formula (Table 1). This might be due to the rougher surface of the mc-Si.

TABLE 1. Structural properties of ZnO layers on all substrates

Sample	d_{0002} (Å)	$2\theta_{(0002)}$	D(nm)
Standard	2.601	34.43	-
ZnO/Glass	2.589	34.60	13.9
ZnO/c-Si	2.586	34.64	21.3
ZnO/mc-Si	2.583	34.68	32

3.2. PHYSICAL PROPERTIES OF ITO

Figure 3 shows the XRD spectra of ITO on different substrates corresponding to a card number ASTM 6-0416 of cubic In_2O_3, with thickness of 300 nm after annealing at 400˚C. None of the spectra shows any characteristic peaks of Sn, SnO and SnO_2, indicating that the tin atoms penetrated substitutionally into the In_2O_3 lattice. It is observed from the Figure 3 that all the ITO thin films are crystalline, having (222) and (400) preferred orientations with stronger (222) Bragg peaks. ZnO-coated specimens have superior crystallinity since the lattice mismatch between the neighboring oxygen–oxygen distance on the closest packed (111) plane of ITO and (0001) plane of ZnO is about 3% [8,20]. In the presence of the ZnO buffer layer, preferred orientation of the crystallinities on glass substrate changes from [100] to [111] direction which can be attributed to the stress regime change from compressive to tensile. Comparing the experimental diffraction peaks with the standard data, slight shifts have been observed in the position of (222) and (400) peaks which are due to the lattice mismatch between the substrate and the thin films. Using ZnO thin films as buffer layers in ITO/Glass and ITO/mc-Si structures reduces the inner pressure stress which decreases the spacing of the lattice planes and increases the position of the XRD peak. Structural characterization of ITO films on bare and ZnO-coated substrates are summarized in Tables 2 and 3.

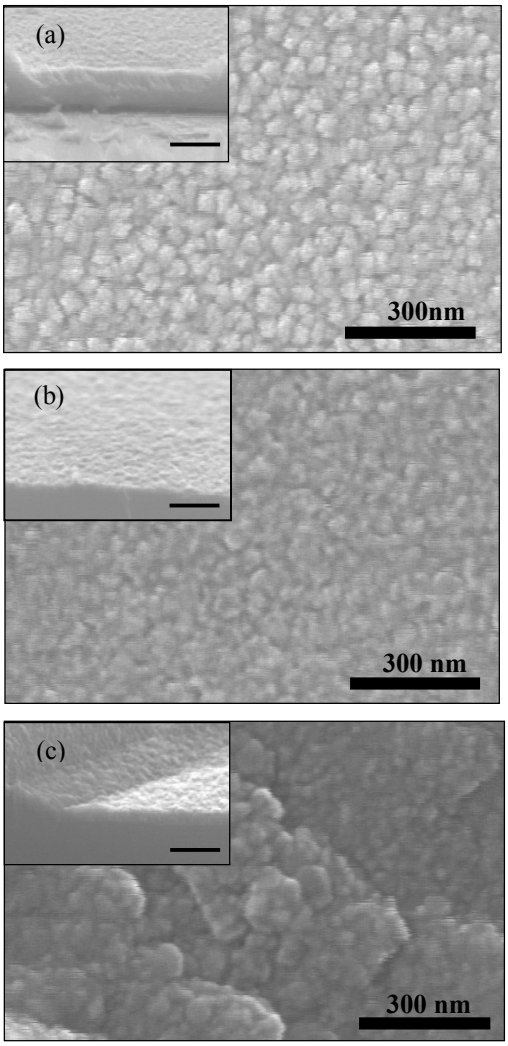

Figure 2. FESEM images of ZnO thin films on (a) glass substrate, (b) monocrystalline Si Wafer, and (c) multi-crystalline Si Wafer (inests show the corresponding cross-sectional image. The scale bars are 300 nm

Lattice distortion values have been calculated by Equation 2 [19]:

$$\frac{\Delta d}{d} = \frac{d_{\exp} - d_{hkl}}{d_{hkl}} \qquad (2)$$

where d is the distance of the adjacent equivalent planes in the ITO lattice corresponding to the XRD spectra's preferred orientation. Introducing the ZnO buffer layer, lattice distortion along the preferred orientation of the crystal decreased and ITO grains were promoted for all kinds of substrates. As can be seen in Tables 2 and 3, in case of not applying the buffer layer, the absolute values of the lattice distortion along the preferred orientation are 0.27%, 0.27% and 0.102% which are decreased to 0.136%, 0.0684% and 0.0342% in the presence of the ZnO buffer layer for glass, c-Si and mc-Si substrates, respectively.

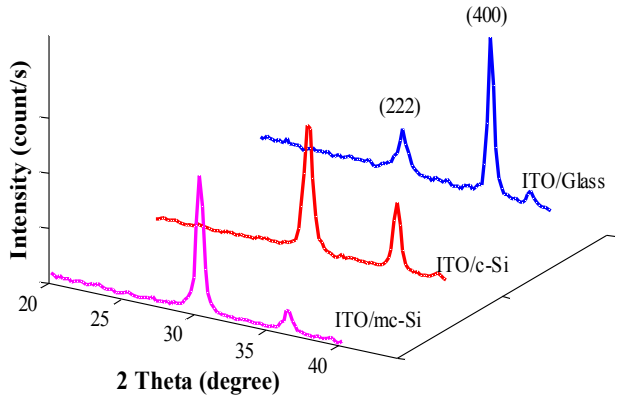

(a)

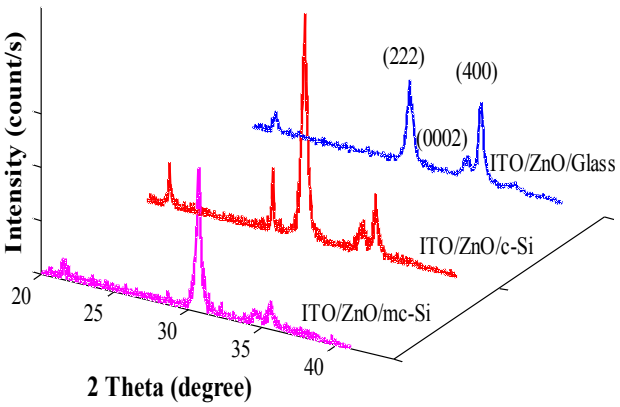

(b)

Figure 3. XRD patterns of ITO thin films on (a) ZnO-coated and (b) uncoated substrates [3,18]

TABLE 2. Structural properties of ITO thin films on ZnO-coated substrates.

Samples	Standard	ITO/ZnO /Glass	ITO/ZnO /c-Si	ITO/ZnO /mc-Si
$d_{(222)}$	2.921	2.925	2.923	2.922
$d_{(400)}$	2.592	2.532	2.534	2.527
$\Delta d_{(222)}/d_{o(222)}$	-	0.00136	0.000684	0.000342
$\Delta d_{(400)}/d_{0(400)}$	-	0.00186	0.00197	-0.000790
$2\theta_{(222)}$	30.56	30.52	30.54	30.55
$2\theta_{(400)}$	35.53	35.40	35.37	35.47
D(nm)	-	16.8	21.2	25.1

TABLE 3. Structural properties of ITO thin films on bare substrates [3,18].

Samples	Standard	ITO/Glass	ITO/c-Si	ITO/mc-Si
$d_{(222)}$	2.921	2.924	2.913	2.924
$d_{(400)}$	2.529	2.536	2.529	2.534
$\Delta d_{(222)}/d_{o(222)}$	-	0.00102	-0.0027	0.00102
$\Delta d_{(400)}/d_{0(400)}$	-	0.0027	0	0.0019
$2\theta_{(222)}$	30.56	30.54	30.66	30.54
$2\theta_{(400)}$	35.53	35.36	35.46	35.38
D(nm)	-	16	10.3	13.7

The resistivity of the specimens was measured by a four point probe system (Table 4). The results demonstrate that the ITO thin film resistivity decreases in the presence of the ZnO buffer layer. The minimum resistivity was obtained from the ITO thin film on the ZnO-coated glass substrate. The superiority of this structure is considered to be originated from its greater vacancy density and higher carrier concentration, which is consistent with its XRD spectrum. It shows that the strongest (400) peak is related to the density of vacancies or carrier concentration. The higher (400) the peak intensity, the lower resistivity is obtained [3].

TABLE 4. Resistivity of ITO thin films on all substrates.

Substrate	**Glass**	**c-Si**	**mc-Si**
$\rho\times10^{-4}$(Ωcm) with ZnO	0.9	3.4	9
$\rho\times10^{-4}$(Ωcm) without ZnO	2.6	7.3	9.4

The transmittance spectra of ITO films deposited on the glass substrate in the presence and absence of the ZnO buffer layers are presented in Fig. 4a. Average transmittances (in the visible range) of uncoated and ZnO-coated structures are 83.5% and 80.6%, respectively. Lower optical transmission in the visible range of the spectrum of the Glass/ZnO/ITO structure can be attributed to partial beam reflection from ITO/ZnO and ZnO/Glass interfaces and more intense optical scattering from longer optical path [18,22].

Absorption of the free electrons even further decreases the transmittance in the infrared portion [23].
For degenerate semiconductors like ITO, the transmittance loss in the near infrared region (NIR) is related to the plasma frequency, around which the transition between transparent to reflectance behavior occurs. The plasma frequency depends on the effective mass of the free electrons and the concentration of charge carriers. The sharpness of the transition from reflectance to transparent behavior also depends upon the electron mobility. Hence, the lower electrical resistance for the ITO/ZnO/Glass structure can be attributed to both higher carrier concentration and/or a higher mobility than ITO grown onto the other substrates. Fig. 4b demonstrates reflectance spectra of the ITO films deposited on glass and c-Si substrates in the presence and absence of ZnO. Utilizing the ZnO buffer layer, the reflectance spectra of the ITO on glass and c-Si substrates show slight changes on their characteristics and there is no influence on the average reflectance value of the layers deposited on mc-Si substrates. Average reflectance values are depicted in Table 5 for comparison.

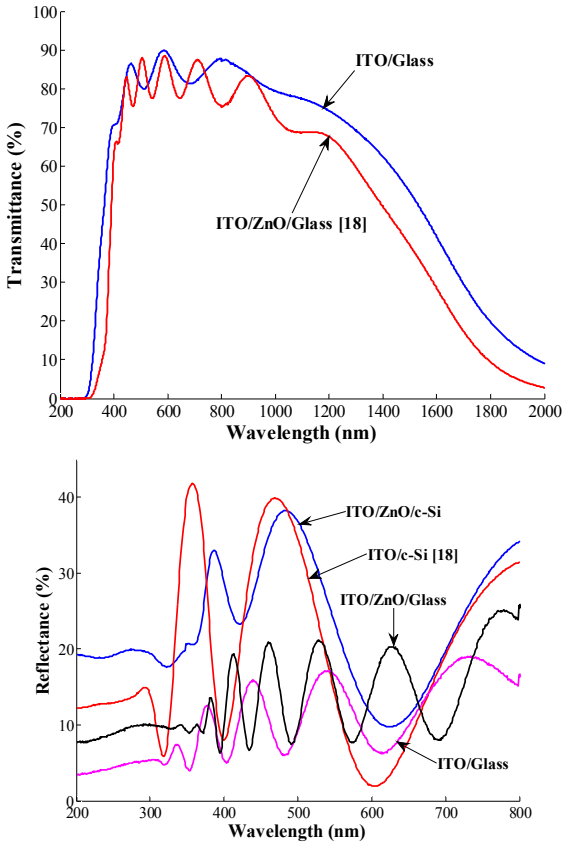

Figure 4. (a) Transmittance spectra of ITO thin films on ZnO-coated and uncoated glass substrates, (b) Reflectance spectra of ITO thin films on ZnO-coated and uncoated glass and c-Si substrates

For textured multicrystalline Si wafers, the surface roughness might be different for different crystallinity types, due to preferential etching of the grain boundaries.
The ZnO buffer layers are utilized to eliminate the effect of surface roughness on ITO physical properties. FESEM images of ITO films on mc-Si with and without ZnO buffer layer are shown in Fig. 5.

TABLE 5. Average reflectance of ITO on Si substrates with and without ZnO buffer layer.

Samples	$\%R_{avg}$ (400-800)	$\%R_{avg}$ (800-2000)
ITO/ZnO/mc-Si	2.8	10
ITO/ZnO/c-Si	24	30
ITO/ZnO/Glass	15.5	19.3
ITO/mc-Si	2.8	10
ITO/c-Si	21	26
ITO/Glass	13	18

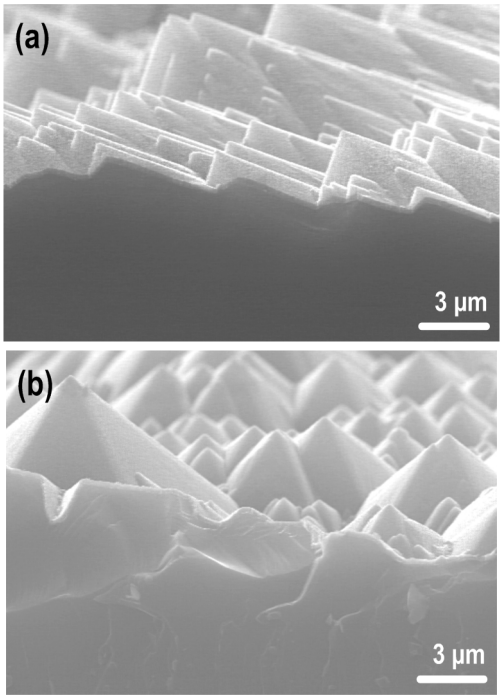

Figure 5. FESEM images of ITO thin films on (a) ZnO-coated and (b) uncoated multi-crystalline Si wafers

Introducing ZnO significantly decreases the roughness of the ITO films from about 3.5 µm to 1.5 µm on mc-Si substrates. The primary surface roughness of the mc-Si wafers used in this work is about 4 µm (before deposition), whereas for ITO films deposited on mc-Si substrates, it reaches 3.5 µm (without buffer layer) and 1.5 µm (with ZnO buffer layer). The rather flat surface in ITO/ZnO/mc-Si structure can be related to the close matching of the ZnO and ITO crystal lattices [24].
Fig. 6 shows plan-view and cross-sectional FESEM images of ITO films on various substrates with and

without ZnO buffer layer. The presence of ZnO promotes the ITO grain sizes, which is consistent with the XRD results (Tables 2 and 3). The largest ITO grains were formed in ITO/ZnO/mc-Si structures. It is believed that large ITO grains formed in this structure have been promoted by large grains of the ZnO under layer. Cross-sectional FESEM images show that the ITO layers grown on ZnO-coated substrates were grown in columnar structures (insets of Figure 6 (a-c)).

AFM analyses have been utilized to study the surface microroughness of the ITO films. Figure 7 depicts AFM images of ITO films on the uncoated and ZnO-coated c-Si substrates as well as Zn-coated c-Si wafers. The surface roughness was deduced from the AFM images in the scanned area of 5μm×5μm. The average surface roughness for the ZnO/c-Si, ITO/ZnO/c-Si and ITO/c-Si structures is 2.757, 3.029 and 5.195 nm, respectively. We noted that the surface roughness of ITO films decreased when deposited on ZnO-coated substrates, compared to when deposited on the bare c-Si substrates.

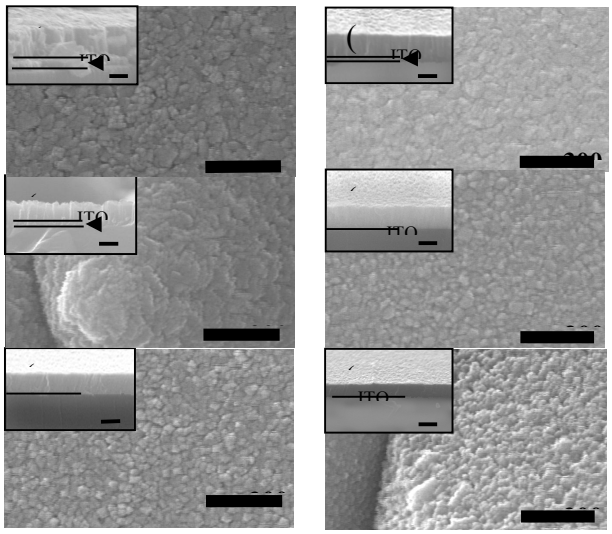

Figure 6. FESEM images of ITO thin films on different substrates: (a) ZnO-coated glass (b) ZnO-coated c-Si and (c) ZnO-coated mc-Si (d) uncoated glass (e) uncoated c-Si, and (f) uncoated mc-Si substrates (Insets show the corresponding cross-sectional image. The scale bars are 300 nm.)

4. CONCLUSION

ITO films were prepared on three different substrates (glass, c-Si and mc-Si) with and without a ZnO buffer layer. The structural, morphological, electrical and optical properties revealed that ZnO buffer layers have a profound effect on the characteristics of ITO thin films.

XRD results showed that ITO films on mc-Si substrate had the least lattice distortion and prominent crystalline structure. SEM images indicated that the surface roughness of the ITO thin films significantly decreases, especially for mc-Si substrates. Moreover, introducing a ZnO buffer layer promotes the ITO grain sizes and provides a smoother surface. AFM analyses illustrated that the surface microroughness of ITO films is lower when deposited on ZnO-coated c-Si substrates than when deposited on the bare c-Si substrates. ITO films on the bare substrates had resistivity values of 2.6×10^{-4} Ωcm, 7.3×10^{-4} Ωcm and 9.4×10^{-4} Ωcm for glass, c-Si and mc-Si substrates, respectively, whereas the ITO layer on ZnO-coated substrates revealed resistivity values of 0.9×10^{-4} Ωcm, 3.4×10^{-4} Ωcm and 9×10^{-4} Ωcm, showing that electrical characteristics of the ITO layer were improved in the presence of the ZnO buffer layer.

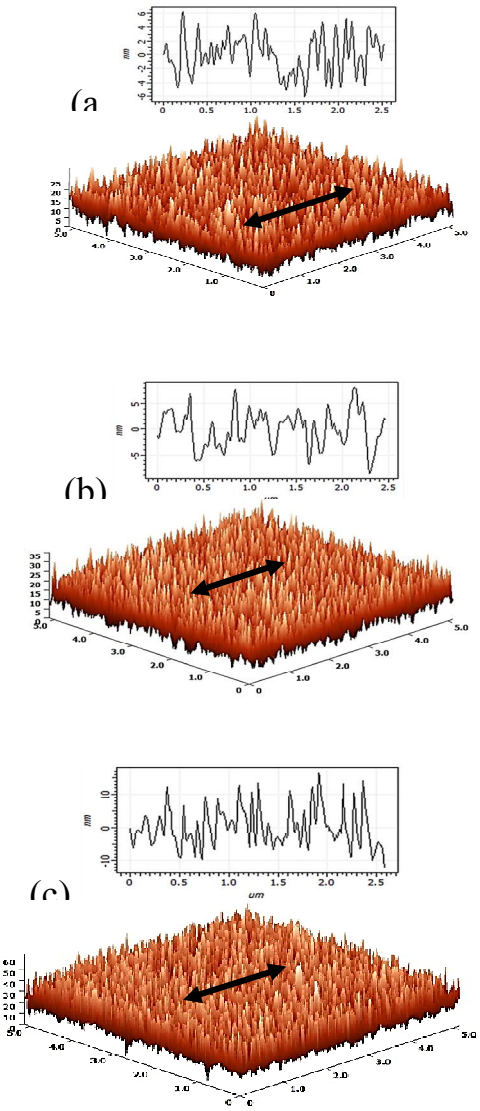

Figure 7. AFM images of (a) ZnO-coated c-Si, (b) ITO layer on ZnO-coated c-Si, and (c) ITO layer on uncoated c-Si structures (Insets show the corresponding roughness profiles.)

In the presence of the ZnO layer, the average transmittance of ITO films decreased, especially in the infrared portion of the spectrum. Although the

transmittance of the structure decreases in the presence of the ZnO buffer layer, it is still suitable for photovoltaic applications. In conclusion, to manufacture low-cost solar cells, transparent conductive oxides and multicrystalline silicon are promising candidate for PV applications.

ACKNOWLEDGMENTS

The author would like to acknowledge Professor E. Asl Soleimani from Thin Film Lab., Faculty of Electrical and Computer Engineering, University of Tehran.

REFERENCES

1. 1. Izumi, H., Ishihara, T., Yoshioka, H., Motoyama, M., "Electrical properties of crystalline ITO films prepared at room temperature by pulsed laser deposition on plastic substrates," ***Thin Solid Films,*** Vol. 411, (2002), 32–35.
2. Caglara, M., Ilican, S., Caglara, Y., Yakuphanoglub, F.,"Boron doped nanostructure ZnO films onto ITO substrate," ***J. Alloys Compd.,*** Vol. 509, (2011), 3177–3182.
3. Manavizadeh, N., Boroumand, F.A., Asl-Soleimani, E., Raissi, F., Bagherzadeh, S., Khodayari, A., Rasouli, M. A., "Influence of substrates on the structural and morphological properties of RF sputtered ITO thin films for photovoltaic application," ***Thin Solid Films,*** Vol. 517, (2009), 2324–2327.
4. Purica, M., Iacomi, F., Baban, C., Prepelita, P., Apetroaei, N., Mardare, D., Luca, D., "Investigation of structural properties of ITO thin films deposited on different substrates," ***Thin Solid Films,*** Vol. 515, (2007), 8674–8678.
5. Sun, X. W., Wang, L. D., Kwok, H. S., "Improved ITO thin films with a thin ZnO buffer layer by sputtering," ***Thin Solid Films***, Vol. 360, (2000), 75-81.
6. Meng, L.-J., Dos Santo, M. P., "Influence of the target-substrate distance on the properties of ITO films prepared by rf reactive magnetron sputtering," ***J. Vac. Sci. Technol. A***, Vol. 18(4), (2000), 1668-1671.
7. Hong, R., Shao, J., He, H., Fan, Z., "Enhancement of Near-Band-Edge Photoluminescence of ZnO Thin Films in Sandwich Configuration at Room Temperature," ***J. Appl. Phys.,*** Vol. 99, (2006), 093520-093523.
8. Vinodkumar, R., Lethy, J. K., Beena, D., Detty, A. P., Navas, I., Nayer, U. V., Mahadevan Pillai, V. P., Ganesan, V., Reddy, V. R., "Effect of ITO buffer layers on the structural, optical and electrical properties of ZnO multilayer thin films prepared by pulsed laser deposition technique," ***Solar Energy Materials & Solar Cells***, Vol. 94, (2010), 68-74.
9. Herrero, J., Guillen, C., "Improved ITO thin films for photovoltaic applications with a thin ZnO layer by sputtering," ***Thin Solid Films,*** Vol. 451–452, (2004), 630–633.
10. Seong, C.-H., Shin, Y. –J., Jang, G. –E., "Effect of ZnO Buffer Layers on the Crystallization of ITO Thin Film at Low Temperature," ***Transaction on electrical and electronic materials,*** Vol. 13(4), (2012), 208-211.
11. Ma, Z.Q., He, B., "Solar Cells - Thin-Film Technologies", chapter 6:TCO-Si Based Heterojunction Photovoltaic Devices, Publisher: InTech, Chapters, 468 pages, November 02, 2011.
12. Melvin David Kumar, M., Yun, J.-H., Kim, J., "Metal/Semiconductor and Transparent Conductor/ Semiconductor Heterojunctions in High Efficient Photoelectric Devices: Progress and Features," ***International Journal of Photoenergy,*** Vol. 2014, Article ID 160379, 14 pages.
13. Plumer, J. D., Deal, M. D., Griffin, P., "Silicon VLSI Technology: Fundamentals, Practice and Modeling," Prentice Hall, Inc., 2000.
14. Manavizadeh, N., Khodayari, A., Asl-Soleimani, E., Bagherzadeh, S., Maleki, M., "Structural properties of post annealed ITO thin films at different temperatures," ***Iran J. Chem. Chem. Eng.***, Vol. 28(2), (2009), 57-61.
15. Guillén, C., Herrero, J., "Polycrystalline growth and recrystallization processes in sputtered ITO thin films," ***Thin Solid Films***, Vol. 510, (2006), 260-264.
16. Matsubara, K., Fons, P., Iwata, K., Yamada, A., Niki, S., "Room-temperature deposition of Al-doped ZnO films by oxygen radical-assisted pulsed laser deposition," ***Thin Solid Films,*** Vol. 422, (2002), 176–179.
17. Lee, J. B., Kwak, S. H., Kim, H. J., "Effects of Surface Roughness of Sub-strates on the c-Axis Preferred Orientation of ZnO Films De-posited by r.f. Magnetron Sputtering," ***Thin Solid Films,*** Vol. 423, (2003), 262–266.
18. Manavizadeh, N., Khodayari, A., Asl Soleimani, E., Bagherzadeh, S., "A Study of ZnO Buffer Layer Effect on Physical Properties of ITO Thin Films Deposited on Different Substrates," ***Iranian Journal of Chemistry and Chemical Engineering,*** Vol. 31(1), (2012), 37-42.
19. Cullity, B. D., Elements of X-ray Diffractions, Addison-Wesley, Reading, MA, 1978.
20. Yi, C. H., Yasui, I., Shegesato, Y., "Oriented Tin-doped Indium oxide-films on [001] preferred oriented polycrystalline ZnO films," ***Jpn. J. Appl. Phys.***, Vol. 1(34), (1995), 1638–1642.
21. Qiao, Z., Mergel, D., "Comparison of radio-frequency and direct-current magnetron sputtered thin In_2O_3:Sn films," ***Thin Solid Films***, Vol. 484, (2005), 146-153.
22. Wong, F. L., Fung, M. K., Tong, S. W., Lee, C. S., Lee, S. L., "Flexible organic light-emitting device based on magnetron sputtered indium-tin-oxide on plastic substrate," ***Thin Solid Films***, Vol. 466, (2004), 225-230.
23. Meng, L. J., Crossar, E. ,"Indium–tin-oxide thin film prepared by microwave-enhanced dc reactive magnetron sputtering for telecommunication wavelengths," ***Thin Solid Films,*** Vol. 422, (2002), 80-86.
24. Kong, B. H., Mohanta, S. K., Kim, D. C., Cho, H. K., "Optical and structural properties of ZnO thin films grown on various substrates by metalorganic chemical vapor deposition," ***Phys. B*** (Amsterdam, Neth.), Vol. 401-402, (2007), 399-403